

protect photoreceptors against phototoxicity [13]. However, suitable devices that specifically deliver neurotrophic factors continuously to the retina and with minimal invasiveness have yet to be developed. Therefore, we aimed to develop a membrane-based capsule that is implantable on the sclera (Fig. 1A) and would prolong the controlled delivery of BDNF or other protein-type drugs to the retina with zero-order kinetics. The designed capsule consists of two parts, a molded triethylene glycol dimethacrylate (TEGDM) reservoir to contain the drug and a new type of controlled-release membrane sealed around the top of the reservoir (Fig. 1B). TEGDM is a biomedical material that has been clinically used as a dental filler for the restoration of teeth [14]. The controlled-release membrane was produced by photopolymerizing a mixture of polyethylene glycol dimethacrylate (PEGDM) and collagen microparticles (COLs) (PEGDM/COL membrane). PEGDM has been successfully used by us [15] and several other groups [16,17] both *in vitro* and *in vivo* as a bio-inert scaffold material that can be easily molded into different substrate shapes and then annealed by UV crosslinking. The COLs are hydrogels containing a chemically crosslinked 0.8% (w/v) collagen network [18], which is permeable to molecules with molecular weights of <200 kDa. Drugs diffuse through the interconnected COLs embedded in the membrane. Additionally, the capsule can contain various formulations and dosages of a drug so that it can be used for many different biomedical applications. Herein, we report the fabrication, characterization, and implantation on rabbit sclerae of this transscleral

drug-delivery device and demonstrate its applicability for the administration of protein-type drugs to the retina.

## 2. Materials and methods

### 2.1. Fabrication of the PEGDM/COL membrane

Mixtures (900  $\mu$ l) of PEGDM prepolymer ( $M_n$  750, Aldrich), 1% 2-hydroxy-2-methylpropiophenone, and COLs at concentrations of 0, 100, 300, or 500 mg/ml were poured individually into acrylic molds ( $3 \times 3 \times 0.1$  cm) and photopolymerized with UV light that had an intensity of 11.5 mJ/cm<sup>2</sup> for 90 s (Lightningcure LCS, Hamamatsu Photonics) to produce membranes with thicknesses of 100  $\mu$ m. COLs (average diameter, 8.7  $\mu$ m) were prepared as described [18]. Briefly, 10 ml of a 1% (w/v) collagen solution (Nippon Meat Packers) was emulsified in 50 ml of liquid paraffin containing 0.3% (v/v) surfactant and stirred (600 rpm) at room temperature for 5 min. To crosslink the collagen, 1 ml of 50% (v/v) water-soluble carbodiimide (Dojindo) in water was added to the emulsified mixture and stirred (600 rpm) for 1 h. Then, 50 ml of 50% (v/v) ethanol was added into the mixture and mixed for 5 min to separate the COLs from the oil phase. The mixture was centrifuged at  $3000 \times g$  for 5 min, and the supernatant was discarded. Ethanol (50% v/v) was mixed with the COL pellet, and then the suspension was centrifuged ( $3000 \times g$  for 5 min). After removing the supernatant, phosphate-buffered saline (PBS) was mixed with the COL pellet and then the suspension was centrifuged ( $3000 \times g$  for 5 min). This procedure was repeated 3 times to remove residual ethanol.

### 2.2. Preparation of drug formulations

Three formulations that contained the drug mimic, 40-kDa fluorescein isothiocyanate dextran (FD40) plus PBS ( $F_{sol}$ ), in COLs ( $F_{col}$ ), or in COLs pelletized with PEGDM ( $F_{pel}$ ) were prepared. For the preparation of  $F_{sol}$ , FD40 (Sigma) was dissolved in PBS at a concentration of 10 mg/ml. For the preparation of  $F_{col}$ , PBS solutions of

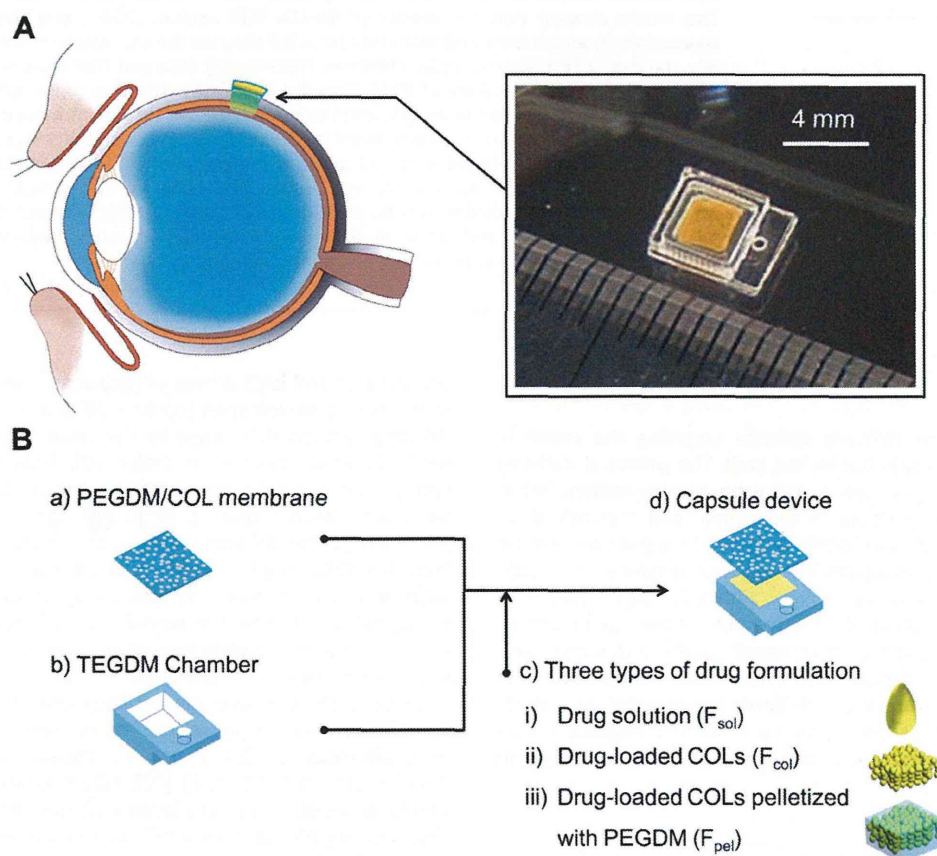


**Fig. 1.** (A) A transscleral drug-delivery device, designed for the administration of protein-type drugs. The photograph shows a capsule that contained FD40-loaded COLs pelletized with PEGDM and has a hole for suturing the capsule onto the sclera. (B) The capsule consists of a drug reservoir made of TEGDM and a controlled-release membrane made of photopolymerized PEGDM that contains COLs (PEGDM/COL membrane), which are the route for drug permeation. The capsule was designed so that various drug formulations could be contained in the reservoir.



COLs, which were obtained by centrifugation at  $3000 \times g$  for 30 min, were stirred in an equal volume of PBS that contained FD40 (20 mg/ml) for 24 h, and then the COLs were washed and centrifuged ( $3000 \times g$  for 5 min) three times with PBS. For the preparation of  $F_{\text{pel}}$ , the FD40-loaded COLs in PBS (20 mg/ml FD40) were mixed with an equal volume of the PEGDM prepolymer and UV cured for 3 min. All drug formulations had the same amount of FD40 (10 mg/ml).

### 2.3. Fabrication of the capsule

A schematic of the capsule fabrication is shown in Fig. 1B. A polydimethylsiloxane master mold for the reservoir was first fabricated via a micro-fabrication technique that used an AutoCAD design and a micro-processing machine (Micro MC-2, PMT Co.). TEGDM prepolymer ( $M_w$  286.3; Aldrich) was UV cured in the mold for 3 min and peeled off to obtain a TEGDM reservoir. After loading a drug, the membrane was sealed to the reservoir by UV curing TEGDM prepolymer, which in polymerized form served as the adhesive, for 3 min.

### 2.4. SEM analysis

Samples were fixed with 2.5% glutaraldehyde and dehydrated first with ethanol and, subsequently, with isoamyl acetate. The samples were then dried fully in a critical point dryer (HCP-2; Hitachi Koki), coated with Pt using an ion coater (L350S-C; Anelva), and subjected to SEM. The SEM apparatus (VE-9800; Kyence) was operated at 5–20 kV.

### 2.5. In vitro release study

Modified Transwells were prepared by replacing their original porous membranes with PEGDM/COL membranes of various compositions (Fig. S2). Each drug formulation (100  $\mu$ l) was placed in a Transwell and the complete systems were incubated in 400  $\mu$ l of PBS at 37 °C. To estimate the amounts of FD40 that had diffused out of the Transwells, the fluorescent intensities of the PBS solutions were measured spectrofluorometrically (Fluoroscan Ascent; Thermo). For the release study that used recombinant human BDNF (rhBDNF), the capsules (reservoir interior,  $5 \times 5 \times 2.2$  mm; capsule exterior,  $10 \times 10 \times 2.4$  mm) were each filled with 40  $\mu$ l of rhBDNF-loaded COLs in PBS and sealed with a membrane with a COL concentration of 0, 100, 300, or 500 mg/ml, and incubated in 1 ml of PBS at 37 °C. The amount of released rhBDNF was measured using the reagents of a BDNF-ELISA kit (Invitrogen) according to the manufacturer's instructions. Each test result is reported as the mean  $\pm$  SD of three samples.

### 2.6. Western blotting

Immortalized retinal ganglion cells (RGC5 cells; a generous gift from Dr. N. Agarwal, University of North Texas Health Science Center, Fort Worth, TX) were maintained in Dulbecco's modified Eagle's medium (DMEM) (1 g glucose/l, Gibco) containing 10% fetal bovine serum (FBS; Gibco), L-glutamine (4 mM, Gibco), and a penicillin (100 U/ml)/streptomycin (100 mg/ml) solution (Sigma). RGC5 cells were plated into culture dishes (diameter; 60 mm, TPP) at a density of  $1 \times 10^4$  cells/cm<sup>2</sup> and incubated in DMEM for 24 h. After starving the cells in DMEM that did not contain FBS (DMEM-f) for 12 h, the cells were exposed to conditioned DMEM-f that contained rhBDNF that had been released from a capsule into the medium (see below) or that had been spiked with rhBDNF (0, 0.1, 1, and 10 ng/ml) for 1 h. Cells were then scraped from the culture support and lysed with the reagents of a ProteoJET Cell Lysis kit (CosmoBio). Protein concentrations were determined using BCA protein assay kit reagents (Pierce). Electrophoresis was performed using 4–15% Tris-glycine gels (Biorad). Proteins were transferred to PVDF membranes using a semidry transferring system (Biorad). The membranes were blocked with 5% ECL blocking agent (GE Healthcare) and then incubated with a primary antibody against phosphorylated MAPK (1:1000; Cell Signaling) and subsequently with the secondary antibody, horseradish peroxidase-linked IgG (1:5000; Cell Signaling). After stripping the membranes of the antibodies for 10 min using the reagents of a Western Re-Probe kit (Jacksun Biotech), the membrane was probed, in a similar manner, for total MAPK (anti-MAPK antibodies, 1:1000; Cell Signaling). Bands were visualized using an enhanced chemiluminescence system (ECL Plus, GE Healthcare). Conditioned media were prepared as follows. Capsules that contained rhBDNF-loaded COLs were incubated in DMEM-f at 37 °C. The medium was replaced with fresh DMEM-f at day 3 and at week 1, 2, 3, and 4.

### 2.7. Implantation study

We used the eyes of six rabbits, each of which weighed between 1.8 and 2.5 kg. All animals were handled in accordance with the ARVO Statement for the Use of Animals in Ophthalmic and Vision Research after receiving approval from the Institutional Animal Care and Use Committee of the Tohoku University Environmental & Safety Committee (No.22MdA-220). The rabbits were anesthetized with ketamine hydrochloride (35 mg/kg) and xylazine hydrochloride (5 mg/kg). Their ocular surfaces were anesthetized with a topical instillation of 0.4% oxybuprocaine hydrochloride. A paralimbal conjunctival incision was made 5–8 mm from the

temporal limbus. The capsules, which were loaded with  $F_{\text{pel}}$ , were sutured onto the left eyes at the sclerae with 10-0 nylon. The right eyes served as controls. At the third day of implantation, fluorescent images were captured using a handheld retinal camera for fluorescein angiography (Genesis-D, Kowa) to document the fluorescence distributions around the capsules and the sclerae. After implantation for 1 month, capsules from three rabbits were carefully removed and subjected to SEM. For histological examination, the other three rabbits were killed with an overdose of pentobarbital sodium 3 days after implantation, and their eyes were enucleated and frozen immediately in liquid nitrogen. After mounting the cryostat sections in a medium that contained 4,6-diamidino-2-phenylindole (Vectashield, Vector Lab), the distribution of FD40 was observed by fluorescent microscopy (DMI6000B, Leica).

### 2.8. Statistical analysis

Experimental data are presented as means  $\pm$  SDs. The results were evaluated by the Student *t*-test. Differences were considered significant if  $P < 0.05$ .

## 3. Results and discussion

### 3.1. Device fabrication

The capsule consists of a separately fabricated PEGDM/COL membrane and a TEGDM reservoir (Fig. 1B). The membrane was prepared by UV curing a mixture of PEGDM and COLs. PEGDM is almost impermeable to macromolecules with molecular weights  $>40$  kDa (see below); therefore, the COLs provide the route for drug permeation. Scanning electron microscopy (SEM) images were acquired to visualize the surfaces of membranes with different COL concentrations. The COLs are the round particles seen in Fig. 2A–C, and the surface density of these particles is proportional to the concentration of COLs in the corresponding unpolymerized PEGDM/COL mixture (Fig. S1). Additionally, cross-sectional SEM images showed the presence of interconnecting COLs when the COL concentration was  $>300$  mg/ml (Fig. 2D–F). The interconnecting COLs increased in density with the concentration of the COLs. Therefore, we assumed that the drug-release rate could be controlled by changing the COL density in the membrane. Because, conventionally, semipermeable membranes are made by forming pores within the membrane i.e., solvent casting/salt leaching [19], phase separation [20], emulsion freeze-drying [21], and bubble formation [22], our method is different and therefore pioneering. For this type of membrane, there is no need to remove remaining porogens (COLs) after polymerization because the COLs act as the route for drug release.

The TEGDM reservoir was microfabricated using a polydimethylsiloxane master mold. Because photopolymerized TEGDM is impermeable to macromolecules (see below), the reservoir is a barrier that forces unidirectional drug release. After loading the drug, the membrane was placed over the reservoir and TEGDM prepolymer was UV cured along the reservoir/membrane intersection to provide a seal. Cross-sectional SEM images indicated that a tight seal was formed (Fig. 2G). The drug mimic, FD40 in PBS, did not leak from a capsule that consisted of a standard TEGDM reservoir and a PEGDM membrane that lacked COLs; therefore, the capsule had been completely sealed. The capsule was designed to contain various drug formulations and dosages. In this study, sustained-release drug formulations were encapsulated to prolong drug release by limiting the rate of drug dissolution within the reservoir (see below).

### 3.2. Release controllability

To demonstrate that drug release could be controlled by both the membrane and the drug formulation, modified Transwell inserts were each fitted with a membrane of defined COL concentration (Fig. S2) and loaded with one of three formulations: FD40 in PBS ( $F_{\text{sol}}$ , Fig. 3A), FD40 in COLs ( $F_{\text{col}}$ , Fig. 3B), or FD40 in COLs



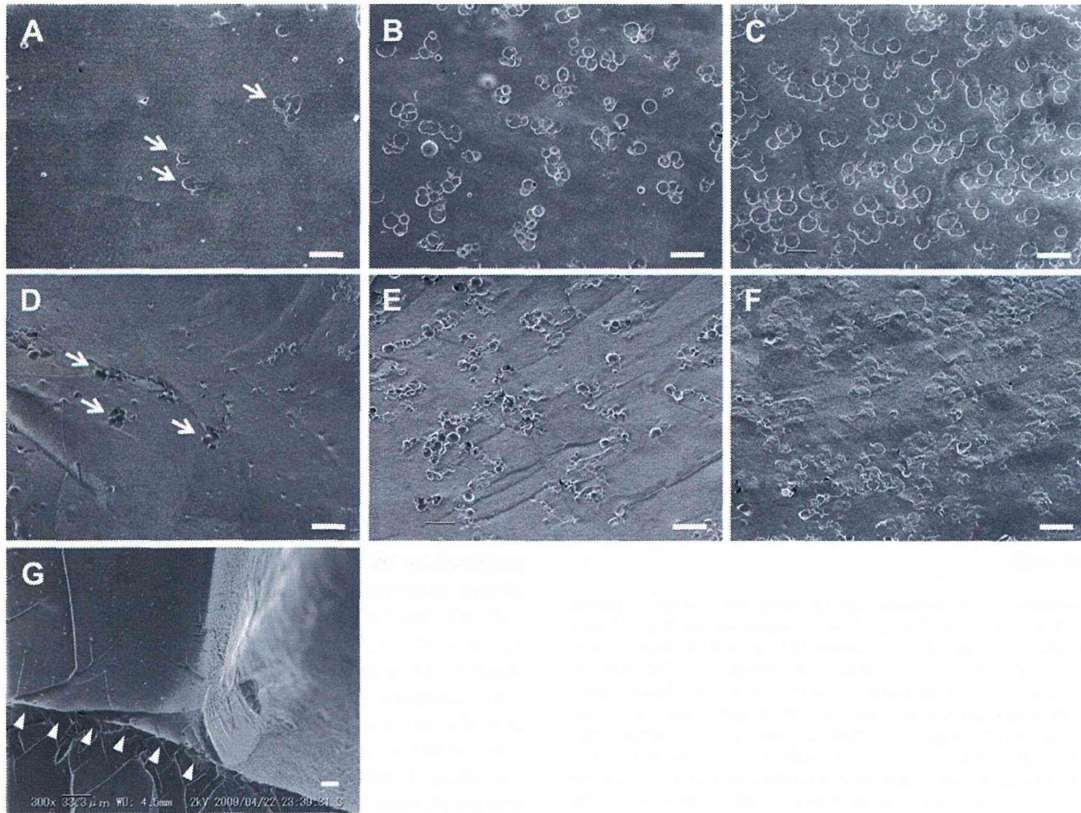


**Fig. 2.** Representative SEM images of (A–C) the surface and (D–F) cross sections of PEGDM/COL membranes that had COL concentrations of (A, D) 100 mg/ml, (B, E) 300 mg/ml, and (C, F) 500 mg/ml. The COLs are the round particles that form interconnecting structures throughout the membrane. Arrows point to COLs embedded in the membranes. (G) A cross-sectional SEM image of the capsule seal site that shows the formation of a tight seal. Arrowheads point to the seal site between the membrane and the capsule exterior. Bars: 20  $\mu$ m.

pelletized with PEGDM (COL/PEGDM pellet) ( $F_{\text{pel}}$ , Fig. 3C). The COLs and the COL/PEGDM pellets, designed to be sustained-release drug formulations, were suspended in PBS. After placing the Transwells in PBS, FD40 release was monitored by assessing the increase in fluorescence in the external PBS solution with time. The results showed that the release of FD40 was always dependent on the COL concentration (Fig. 3A–C), which indicated that FD40 travelled

through the membrane-embedded COLs. At the COL concentration of 100 mg/ml, the release kinetics was almost the same as the control (0 mg COL/ml). As shown by SEM analysis, almost no interconnected COLs existed in the 100 mg COL/ml membrane. When the membranes had been prepared with a COL concentration of 300 mg/ml, drug release followed zero-order kinetics. Additionally,  $F_{\text{col}}$  and  $F_{\text{pel}}$  behaved as sustained-release drug

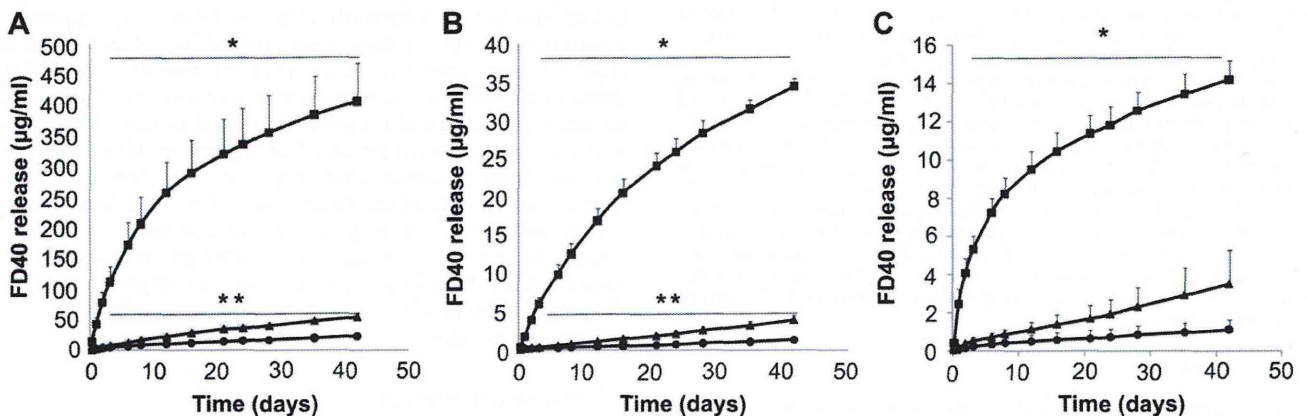


**Fig. 3.** Release of FD40 *in vitro*. The permeability of FD40 through PEGDM/COL membranes was studied using modified Transwells for which the PEGDM/COL membranes replaced the original Transwell membranes. The dependence of the release kinetics on the initial COL concentration for (A) FD40 in PBS ( $F_{\text{sol}}$ ), (B) FD40-loaded COLs in PBS ( $F_{\text{col}}$ ), and (C) FD40-loaded COLs pelletized with PEGDM in PBS ( $F_{\text{pel}}$ ). The concentrations of the COLs were 100 mg/ml (circles), 300 mg/ml (triangles), and 500 mg/ml (squares). The release rate for FD40 through a membrane that did not contain COLs was almost the same as one that contained COLs at a concentration of 100 mg/ml. Error bars represent the standard deviations of three samples (error bars that are not visible are smaller than the symbols). The Means  $\pm$  SDs are shown. \* $P < 0.05$  for 300 mg/ml vs. 500 mg/ml \*\* $P < 0.05$  for 100 mg/ml vs. 300 mg/ml.



formulations as they fine-tuned the release of FD40 in comparison with that of  $F_{sol}$ , perhaps because the COL and COL/PEGDM pellets, which cannot permeate the membrane, caused the reservoir solutions to have lower FD40 concentrations, which, in turn, decreased the steepness of the FD40 gradient from the reservoir to the exterior PBS solution. Therefore, the  $F_{col}$  and  $F_{pel}$  formulations, as sustained drug-release systems, improved the ability to control FD40 release by limiting the rate of FD40 dissolution, with the membrane controlling the diffusion rate via the COL tunnels. Consequently, the release of a drug can be controlled by the COL concentration in the membrane and the drug formulation.

### 3.3. Release mechanism

To further characterize the FD40 diffusion mechanism, we determined the diffusion coefficients for FD40 through 0.8% (w/v) crosslinked collagen ( $D_c$ ), PEGDM ( $D_p$ ), TEGDM ( $D_t$ ), and water ( $D_w$ ).  $D_c$ ,  $D_p$ , and  $D_t$  were calculated using the FD40 diffusion rates through the gels (Fig. S3), and  $D_w$  was calculated using the Stokes–Einstein equation [23]. Because  $D_c$  ( $45.2 \mu\text{m}^2/\text{s}$ ) was 1000 times larger than  $D_p$  ( $0.045 \mu\text{m}^2/\text{s}$ ) and was smaller than  $D_w$  ( $67.9 \mu\text{m}^2/\text{s}$ ), it appears that FD40 diffused through interconnected COLs in the membranes. If the COLs in the membrane are not interconnected, dead-ends are probably present that would inhibit the rate of drug release to the outside. However, once the COL density increases above a permeation threshold ( $>100 \text{ mg COL/ml}$ ), which was estimated by SEM as noted above (Fig. 2D–F), the COLs should be sufficiently interconnected that the number of dead-ends is reduced, and permeability is thereby increased. Because  $D_t$  was zero, FD40 cannot diffuse through the TEGDM reservoir, which enables unidirectional drug release.

### 3.4. In vitro BDNF release and bioactivity

To evaluate the release of the neurotrophic factor rhBDNF, capsules were filled with COLs that contained the protein and were tightly sealed with a membrane with a COL concentration of 0, 100, 300, or 500 mg/ml (Fig. 4A) presents the zero-order kinetic profiles found for rhBDNF release during a 6-week assay period. Apparently, the release kinetics of rhBDNF can be fine-tuned by varying the concentration of the COLs in a membrane in much the same manner as was found for FD40. Additionally, media that had been preincubated with capsules that contained rhBDNF induced the phosphorylation of mitogen-activated protein kinase (MAPK) in RGC5 cells when incubated with those cells as shown by western

blotting of the cell extracts (Fig. 4B). BDNF is known to upregulate the expression of phosphorylated MAPK in retinal tissue [24]. In the present study, rhBDNF was found to phosphorylate MAPK in RGC5 cells in a dose-dependent manner by incubating the cells with media spiked with rhBDNF (Fig. 4C), which demonstrated that, when released from the capsule, rhBDNF retained its full activity.

Among the known neurotrophic factors, BDNF is the most potent survival factor for damaged retinal ganglion cells [10,25,26]. However, BDNF is currently administered to the retina by intravitreal or subretinal injections in PBS [26], adenovirus vectors containing the BDNF gene [26,27], or genetically modified cells that secrete BDNF [13,28]. Direct injections, however, result in extreme patient discomfort and complications arise caused by repeated injections or surgical procedures [2]. Because our capsule can contain various drug formulations, the encapsulation of the adenovirus vectors and the genetically modified cells might be possible and, as such, would represent a less invasive path than is currently available.

### 3.5. Implantation study

Our next challenge was to evaluate the capsule's ability to deliver a protein-type drug to the retina via the sclera. Capsules that had a reservoir ( $2.6 \times 2.6 \times 0.6 \text{ mm}$ ) filled with  $F_{pel}$  were sutured to the sclerae of three rabbits' left eyes with 10-0 nylon (Fig. 5A). The capsules abutted the sclerae but did not penetrate the conjunctivae or adjacent areas. Fig. 5B shows a fluorescent image of FD40 within a capsule, and Fig. 5C shows the release of FD40 locally at the sclera but not at the conjunctiva. This unidirectional release should reduce drug elimination by conjunctival lymphatic/blood clearance, thereby resulting in more effective delivery to the retina [29]. One month after implantation, the capsules remained sutured and neither the PEGDM of the membranes (Fig. 5D) nor the reservoirs had eroded (Fig. S4). The COLs in the membranes also survived with little biodegradation (Fig. 5D), most likely because the collagen molecules were stabilized by chemical crosslinking [18]. Although the capsules were loosely covered with connective tissue by the end of the trial, they were easily removed from the implant site. Routine ophthalmological examinations showed no eye-related toxic effects. Intense FD40 fluorescence in the sclerae adjacent to the implantation sites was observed (Fig. 5E). Furthermore, FD40 had migrated to the retinal pigment epithelium (RPE) and adjacent regions (Fig. 5F), which indicated that transscleral delivery of FD40 to the retina had been achieved. To the best of our knowledge, this is the first report that a macromolecule can be delivered to the

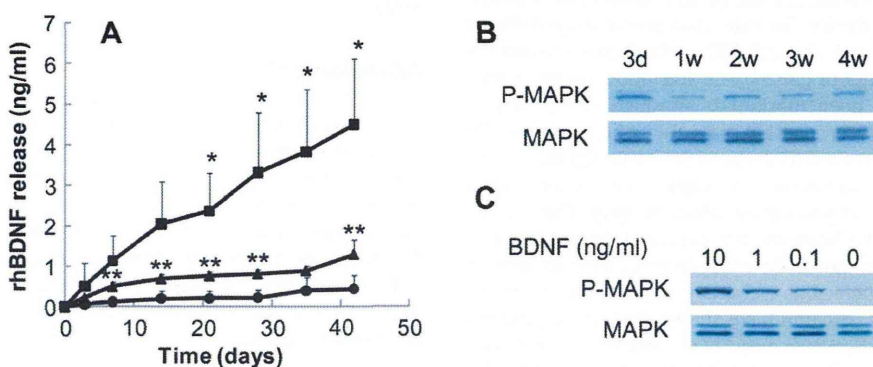


**Fig. 4.** Release of rhBDNF *in vitro*. (A) rhBDNF-loaded COLs were added to capsule reservoirs that sealed with a membrane with a COL concentration of 100 mg/ml (circles), 300 mg/ml (triangles), or 500 mg/ml (squares), and the release of rhBDNF was monitored using the reagents of a BDNF-ELISA kit. The release rate of rhBDNF through a PEGDM/COL membrane that contained 100 mg COL/ml was almost the same as one that contained no COLs. Means  $\pm$  SDs are shown. \* $P < 0.05$  for 300 mg/ml vs. 500 mg/ml \*\* $P < 0.05$  for 100 mg/ml vs. 300 mg/ml. (B) Western blots of RGC5 cells extracts probed with antibody against phosphorylated MAPK (P-MAPK) and total MAPK. (C) The control study showed that rhBDNF could induce MAPK phosphorylation in RGC5 cells in a dose-dependent manner by incubating the cells with media spiked with rhBDNF.



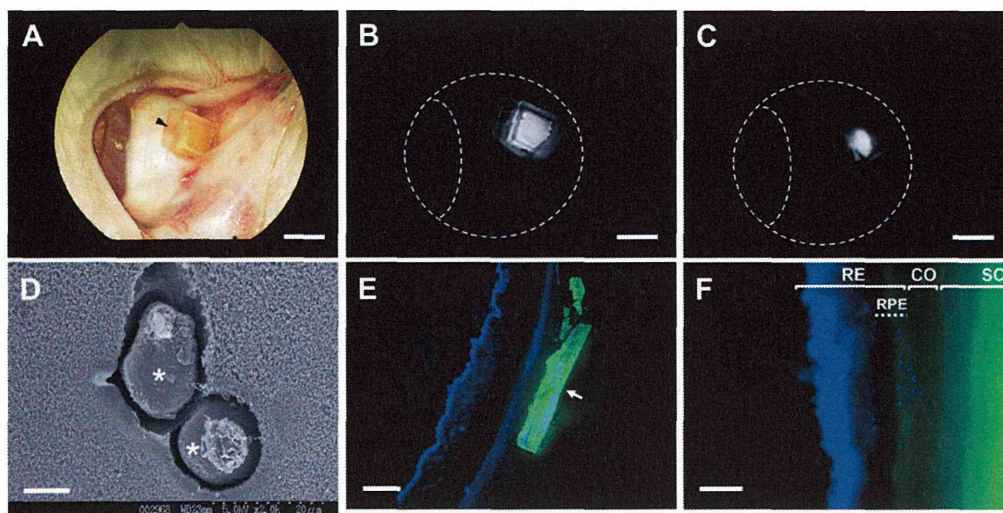


**Fig. 5.** Episcleral implantation of a capsule. (A) Image of a capsule sutured to the sclera of a rabbit eye 3 days after implantation. An arrowhead indicates the suture site. Fluorescent images around the sclera (B) immediately before and (C) after removal of the capsule 3 days after implantation. Fluorescence is visible as the white areas. (D) SEM image of a COL (asterisks) in the membrane of a used capsule that was removed 1 month after implantation. The COLs were not biodegraded. (E, F) The distribution of FD40 (green) in the retina and sclera around the implantation site 3 days after implantation (arrow: capsule). Cell nuclei were stained with 4,6-diamidino-2-phenylindole (blue). FD40 reached the retinal pigment epithelium. Abbreviations: sclera (SC), retinal pigment epithelium (RPE), choroid (CO), and retina (RE). Bars: 4 mm (A, B, and C), 10  $\mu$ m (D), 400  $\mu$ m (E), and 100  $\mu$ m (F).

retina via a reservoir-based transscleral drug-delivery system, although quantification of the drug distribution still needs to be done. Proteins, as large as 50–75 kDa, penetrate into the choroid/RPE upon periorbital injection [30]. Therefore, it may be possible to also deliver BDNF by the transscleral route. Given that the distribution of FD40 was somewhat concentrated at the RPE and adjacent regions, our device may be effective especially for lesions that surround the RPE. The capsule could also be used to deliver anti-angiogenic drugs, e.g., Lucentis and Macugen (for the treatment of age-related macular diseases) [31], to a lesion, e.g., the choroidal neovascular membrane, because delivery by this route will be less invasive and safer than are conventional intravitreal injections. Our non-biodegradable capsule should therefore be suitable for the transscleral delivery of protein-type drugs that require chronic suppressive-maintenance therapy over several weeks or months.

In summary, our capsule design incorporates features, outlined below, that have been absent from intraocular drug-delivery implant systems previously developed. First, the drug release kinetics can be controlled by changing the drug formulation and/or the membrane COL density so that the initial and final bursts are suppressed, which extends the release period. Second, the capsule is a scleral implantable device. To date, two ocular drug-delivery systems, Vitrasert [32] and Retisert [33], which are intravitreal sustained-release implants of ganciclovir and fluocinolone acetonide, respectively, have been marketed. Although these devices release the drugs at relatively constant rates, they must be surgically implanted in and later removed from the vitreous, which may cause complications or patient discomfort. Our capsule can be implanted and removed almost noninvasively by minor surgery. Third, most transscleral drug-delivery systems are designed to deliver low molecular weight drugs; however, ours appears able to deliver drugs of much greater molecular weights, i.e., protein-type drugs. Recent clinical trials and research have shown that many proteins are effective as drugs [9]. However, none of the available devices can deliver protein-type drugs in a controlled-release manner to the retina. Our capsule can be easily modified to accommodate different release rates for protein-type drugs by altering the membrane COL composition and/or drug formulation. Although this report demonstrated the release of only FD40 and BDNF, it should be

possible to load and release low molecular weight drugs, protein-type drugs, and even drugs produced by encapsulated cells. The capsule thus has great potential for use in biomedical applications. Our future work will focus on preclinical animal studies to further assess the safety and effectiveness of the capsule.

#### 4. Conclusion

This study reports the design and testing of a transscleral drug-delivery system that is implantable in the episclera and allows for controlled release of BDNF or other protein-type drugs with zero-order kinetics. Our microfabricated capsule consists of a drug reservoir sealed with a controlled-release membrane that contains interconnected COLs, which are the routes for drug permeation. The drug release kinetics can be controlled by changing the drug formulation and/or the membrane COL density so that the size of the bursts is reduced, which extends the release period. The capsule is designed to contain various drug formulations and dosages, allowing for a wide range of biomedical applications. The device thus has great potential as a conduit for continuous, controlled drug release.

#### Acknowledgments

This study was supported by the Takeda Science Foundation, the Research for Promoting Technological Seeds from the Japan Science and Technology Agency, and the Tohoku University Exploratory Research Program for Young Scientists, and was partially supported by Grants-in-Aid for Scientific Research B (20310070) and for Scientific Research on Priority Areas (21023002, 17659542, 18659508) from the Ministry of Education, Science, and Culture, Japan. Supporting information is available online or from the corresponding author.

#### Appendix

Figure with essential color discrimination. Fig. 4 of this article has parts that are difficult to interpret in black and white. The full



color image can be found in the online version, at doi:10.1016/j.biomaterials.2010.11.006.

## Appendix. Supplementary data

Supplementary data related to this article can be found online at doi:10.1016/j.biomaterials.2010.11.006.

## References

- [1] Hughes PM, Olejnik O, Chang-Lin JE, Wilson CG. Topical and systemic drug delivery to the posterior segments. *Adv Drug Deliv Rev* 2005;57:2010–32.
- [2] Geroski DH, Edelhauser HF. Transscleral drug delivery for posterior segment disease. *Adv Drug Deliv Rev* 2001;52:37–48.
- [3] Ranta VP, Urtti A. Transscleral drug delivery to the posterior eye: prospects of pharmacokinetic modeling. *Adv Drug Deliv Rev* 2006;58:1164–81.
- [4] Ambati J, Adams AP. Transscleral drug delivery to the retina and choroid. *Prog Retin Eye Res* 2002;21:145–51.
- [5] Olsen TW, Edelhauser HF, Lim JI, Geroski DH. Human scleral permeability. Effects of age, cryotherapy, transscleral diode laser, and surgical thinning. *Invest Ophthalmol Vis Sci* 1995;36:1893–903.
- [6] Myles ME, Neumann DM, Hill JM. Recent progress in ocular drug delivery for posterior segment disease: emphasis on transscleral iontophoresis. *Adv Drug Deliv Rev* 2005;57:2063–79.
- [7] Kunou N, Ogura Y, Yasukawa T, Kimura H, Miyamoto H, Honda Y, et al. Long-term sustained release of ganciclovir from biodegradable scleral implant for the treatment of cytomegalovirus retinitis. *J Control Release* 2000;68:263–71.
- [8] McHugh AJ. The role of polymer membrane formation in sustained release drug delivery systems. *J Control Release* 2005;109:211–21.
- [9] LaVail MM, Unoki K, Yasumura D, Matthes MT, Yancopoulos GD, Steinberg RH. Multiple growth factors, cytokines, and neurotrophins rescue photoreceptors from the damaging effects of constant light. *Proc Natl Acad Sci U S A* 1992;89:11249–53.
- [10] Di Polo A, Aigner LJ, Dunn RJ, Bray GM, Aguayo AJ. Prolonged delivery of brain-derived neurotrophic factor by adenovirus-infected Muller cells temporarily rescues injured retinal ganglion cells. *Proc Natl Acad Sci U S A* 1998;95:3978–83.
- [11] Adamus G, Sugden B, Shiraga S, Timmers AM, Hauswirth WW. Anti-apoptotic effects of CNTF gene transfer on photoreceptor degeneration in experimental antibody-induced retinopathy. *J Autoimmun* 2003;21:121–9.
- [12] Faktorovich EG, Steinberg RH, Yasumura D, Matthes MT, LaVail MM. Photoreceptor degeneration in inherited retinal dystrophy delayed by basic fibroblast growth factor. *Nature* 1990;347:83–6.
- [13] Abe T, Yoshida M, Yoshioka Y, Wakusawa R, Tokita-Ishikawa Y, Seto H, et al. Iris pigment epithelial cell transplantation for degenerative retinal diseases. *Prog Retin Eye Res* 2007;26:302–21.
- [14] Kalachandra S. Influence of fillers on the water sorption of composites. *Dent Mater* 1989;5:283–8.
- [15] Hashimoto M, Kaji H, Nishizawa M. Selective capture of a specific cell type from mixed leucocytes in an electrode-integrated microfluidic device. *Biosens Bioelectron* 2009;24:2892–7.
- [16] Lin-Gibson S, Bencherif S, Cooper JA, Wetzel SJ, Antonucci JM, Vogel BM, et al. Synthesis and characterization of PEG dimethacrylates and their hydrogels. *Biomacromolecules* 2004;5:1280–7.
- [17] Weber LM, He J, Bradley B, Haskins K, Anseth KS. PEG-based hydrogels as an in vitro encapsulation platform for testing controlled beta-cell microenvironments. *Acta Biomater* 2006;2:1–8.
- [18] Nagai N, Kumasaka N, Kawashima T, Kaji H, Nishizawa M, Abe T. Preparation and characterization of collagen microspheres for sustained release of VEGF. *J Mater Sci Mater Med* 2010;21:1891–8.
- [19] Meier MM, Kanis LA, Soldi V. Characterization and drug-permeation profiles of microporous and dense cellulose acetate membranes: influence of plasticizer and pore forming agent. *Int J Pharm* 2004;278:99–110.
- [20] Vogelaar L, Lammertink RG, Barsema JN, Nijdam W, Bolhuis-Versteeg LA, van Rijn CJ, et al. Phase separation micromolding: a new generic approach for microstructuring various materials. *Small* 2005;1:645–55.
- [21] Grinberg O, Binderman I, Bahar H, Zilberman M. Highly porous bioresorbable scaffolds with controlled release of bioactive agents for tissue-regeneration applications. *Acta Biomater* 2010;6:1278–87.
- [22] Yoon JJ, Park TG. Degradation behaviors of biodegradable macroporous scaffolds prepared by gas foaming of effervescent salts. *J Biomed Mater Res* 2001;55:401–8.
- [23] Brandl F, Kastner F, Gschwind RM, Blunk T, Tessmar J, Gopferich A. Hydrogel-based drug delivery systems: comparison of drug diffusivity and release kinetics. *J Control Release* 2010;142:221–8.
- [24] Klockner N, Kermer P, Weishaupt JH, Labes M, Ankerhold R, Bahr M. Brain-derived neurotrophic factor-mediated neuroprotection of adult rat retinal ganglion cells in vivo does not exclusively depend on phosphatidylinositol-3'-kinase/protein kinase B signaling. *J Neurosci* 2000;20:6962–7.
- [25] Pernet V, Di Polo A. Synergistic action of brain-derived neurotrophic factor and lens injury promotes retinal ganglion cell survival, but leads to optic nerve dystrophy in vivo. *Brain* 2006;129:1014–26.
- [26] Mansour-Robaey S, Clarke DB, Wang YC, Bray GM, Aguayo AJ. Effects of ocular injury and administration of brain-derived neurotrophic factor on survival and regrowth of axotomized retinal ganglion cells. *Proc Natl Acad Sci U S A* 1994;91:1632–6.
- [27] Martin KR, Quigley HA, Zack DJ, Levkovitch-Verbin H, Kielczewski J, Valenta D, et al. Gene therapy with brain-derived neurotrophic factor as a protection: retinal ganglion cells in a rat glaucoma model. *Invest Ophthalmol Vis Sci* 2003;44:4357–65.
- [28] Harper MM, Adamson L, Blits B, Bunge MB, Grozdanic SD, Sakaguchi DS. Brain-derived neurotrophic factor released from engineered mesenchymal stem cells attenuates glutamate- and hydrogen peroxide-mediated death of staurosporine-differentiated RGC-5 cells. *Exp Eye Res* 2009;89:538–48.
- [29] Robinson MR, Lee SS, Kim H, Kim S, Lutz RJ, Galban C, et al. A rabbit model for assessing the ocular barriers to the transscleral delivery of triamcinolone acetonide. *Exp Eye Res* 2006;82:479–87.
- [30] Demetriades AM, Deering T, Liu H, Lu L, Gehlbach P, Packer JD, et al. Transscleral delivery of antiangiogenic proteins. *J Ocul Pharmacol Ther* 2008;24:70–9.
- [31] Wong TY, Liew G, Mitchell P. Clinical update: new treatments for age-related macular degeneration. *Lancet* 2007;370:204–6.
- [32] Sanborn GE, Anand R, Torti RE, Nightingale SD, Cal SX, Yates B, et al. Sustained-release ganciclovir therapy for treatment of cytomegalovirus retinitis. Use of an intravitreal device. *Arch Ophthalmol* 1992;110:188–95.
- [33] Jaffe GJ, Martin D, Callanan D, Pearson PA, Levy B, Comstock T. Fluocinolone acetonide implant (Retisert) for noninfectious posterior uveitis: thirty-four-week results of a multicenter randomized clinical study. *Ophthalmology* 2006;113:1020–7.

# Preparation and characterization of collagen microspheres for sustained release of VEGF

Nobuhiro Nagai · Norihiro Kumasaka ·  
Takeaki Kawashima · Hirokazu Kaji ·  
Matsuhiko Nishizawa · Toshiaki Abe

Received: 10 November 2009 / Accepted: 2 March 2010 / Published online: 16 March 2010  
© Springer Science+Business Media, LLC 2010

**Abstract** In this study, we prepared injectable collagen microspheres for the sustained delivery of recombinant human vascular endothelial growth factor (rhVEGF) for tissue engineering. Collagen solution was formed into microspheres under a water-in-oil emulsion condition, followed by crosslinking with water-soluble carbodiimide. Various sizes of collagen microspheres in the range of 1–30  $\mu\text{m}$  diameters could be obtained by controlling the surfactant concentration and rotating speed of the emulsified mixture. Particle size proportionally decreased with increasing the rotating speed (1.8  $\mu\text{m}$  per 100 rpm increase in the range of 300–1,200 rpm) and surfactant concentration (3.1  $\mu\text{m}$  per 0.1% increase in the range of 0.1–0.5%). The collagen microspheres showed a slight positive charge of 8.86 and 3.15 mV in phosphate-buffered saline and culture medium, respectively. Release study showed the sustained release of rhVEGF for 4 weeks. Released rhVEGF was able to induce capillary formation of human umbilical vein endothelial cells, indicating the maintenance of rhVEGF bioactivity after release. In conclusion, the results suggest that the collagen microspheres have potential for sustained release of rhVEGF.

## 1 Introduction

Recent studies report that angiogenesis is useful for tissue engineering applications, especially for large tissue formation. Vascular endothelial growth factor (VEGF) has been reported as a potent angiogenic molecule [1]. However, VEGF administered in the body can be degraded and cleared from the body within short time periods, leading to repeated administration [2]. For this reason, many materials for sustained delivery of VEGF have been studied [3, 4]. Microsphere-based drug delivery systems have been receiving increasing attention because they are injectable and are able to deliver multiple drugs [4–7].

Natural polymers such as collagen, gelatin, albumin, and hyaluronic acid have been used for drug delivery system (DDS) materials [8–11]. The advantage of employing such natural polymers is their excellent biocompatibility, compared to that of synthetic polymers. Among natural polymers, collagen exhibits superior biocompatibility because collagen is one of the major components of extracellular matrix and plays important roles in various biological events. Despite the advantages of collagen, little effort has been made to fabricate injectable collagen microspheres for VEGF delivery.

In this study, we prepared the injectable collagen microspheres for sustained release of VEGF using a water-in-oil emulsion system. First, the effects of surfactant concentration and rotating speed in emulsified mixture on the particle diameter were studied. Second, the microscopic observation and surface charge of the collagen microspheres were investigated. Third, we evaluated the release profile of recombinant human VEGF (rhVEGF) from the collagen microspheres. Finally, the bioactivity of rhVEGF released from the collagen microspheres were evaluated using a capillary formation assay of human umbilical vein

---

N. Nagai (✉) · N. Kumasaka · T. Abe  
Division of Clinical Cell Therapy, Center for Translational  
and Advanced Animal Research (CTAAR), Tohoku University  
Graduate School of Medicine, 2-1, Seiryō-machi, Aoba-ku,  
Sendai, Miyagi 980-8575, Japan  
e-mail: nagain@m.tains.tohoku.ac.jp

T. Kawashima · H. Kaji · M. Nishizawa  
Department of Bioengineering and Robotics, Graduate School  
of Engineering, Tohoku University, 6-6-01 Aramaki-Aoba,  
Aoba-ku, Sendai, Miyagi 980-8579, Japan

H. Kaji · M. Nishizawa  
JST, CREST, Sanbancho, Chiyoda-ku, Tokyo 102-0075, Japan

endothelial cells (HUVECs). Here, we demonstrate the method to control the particle diameter of the collagen microspheres in the range of 1–30  $\mu\text{m}$  and characterize the collagen microspheres as a potential DDS material.

## 2 Materials and methods

### 2.1 Reagents

Native collagen from porcine skin was purchased from Nippon Meat Packers (Japan). Liquid paraffin, sorbitan monolaurate (Span 20), water-soluble carbodiimide (WSC), rhVEGF, Dulbecco's modified Eagle's medium (DMEM), and fetal bovine serum (FBS) were purchased from WAKO Pure Chemical Industries (Japan). A VEGF ELISA kit and an antihuman CD31 immunostaining kit were purchased from invitrogen (Japan) and Kurabo (Japan), respectively. HUVECs, human normal dermal fibroblasts (NHDFs), and EGM-2 (growth medium for HUVECs) were purchased from Sanko Jyunyaku (Japan). EGM-2 was supplemented with human epidermal growth factor, hydrocortisone, FBS (2%), VEGF, basic fibroblast growth factor (bFGF), long R insulin-like growth factor-1 (IGF-1), ascorbic acid (Asc), gentamicin sulfate and heparin, as described by the manufacturer. EGM-2 without VEGF, bFGF, IGF-1, Asc, and heparin were prepared for a non-angiogenic medium (EGM) for HUVECs.

### 2.2 Preparation of collagen microspheres

Ten ml of 1% (w/v) collagen solution was emulsified in 50 ml of liquid paraffin containing surfactant at various concentrations (0–1.5% [v/v]) and stirred using a high power mixer (P-2, AsOne, Japan) at various rotating speeds (300–1,200 rpm) at room temperature for 5 min. For crosslinking, 1 ml of 50% (v/v) WSC in water was added to the emulsified mixture and kept stirring for 1 h to form collagen microspheres. Then, 50 ml of 50% (v/v) ethanol was added into the mixture and mixed for 5 min to separate the collagen microspheres from oil phase. The mixture was centrifuged at 3,500 rpm for 5 min and supernatant was removed. Ethanol (50% v/v) was added to the remained collagen pellet and mixed and centrifuged again (3,500 rpm, 5 min). After removal of supernatant, phosphate buffered-saline (PBS) was added to the collagen pellet and mixed and centrifuged (3,500 rpm, 5 min). This procedure was repeated 3 times to remove residual ethanol. The collagen microspheres for the experiments of VEGF impregnation, zeta potential, microscopic observation, in vitro release assay, and capillary formation assay were prepared under the conditions of the surfactant concentration of 0.3% and the rotating speed of 600 rpm.

### 2.3 VEGF impregnation in collagen microspheres

Impregnation of rhVEGF in the collagen microspheres was performed by immersing the collagen microspheres in the 1  $\mu\text{g}/\text{ml}$  rhVEGF solution in PBS for 24 h at 4°C. The microspheres loaded rhVEGF were centrifuged at 3,500 rpm for 5 min and supernatant was removed. PBS was added to the collagen pellet and mixed and centrifuged (3,500 rpm, 5 min). This procedure was repeated 3 times to remove residual rhVEGF.

### 2.4 Particle size

The particle size of the collagen microspheres were measured by hand count. The collagen microspheres were stirred in PBS overnight to disperse homogeneously. The pictures of the collagen microspheres were taken through a microscope (DMI6000B, Leica, Japan) and the diameters of the microspheres of at least 500 microspheres were measured by hand count.

### 2.5 Viscosity

The viscosities of liquid paraffin and collagen solutions (0.5, 1, and 1.5% [w/v]) at various temperatures were measured using a viscometer (viscostick; Shiro Industry, Japan).

### 2.6 Zeta potential

The surface charge of the collagen microspheres was determined by measuring the electrophoretic mobility using a Zetasizer (Nano ZS; Sysmex, Japan). The measurements were performed in PBS and EGM to investigate the solvents dependency of the zeta potential. A Smoluchowsky model was used to calculate the zeta potential values from the electrophoretic mobility. All measurements were carried out at 25°C in triplicate.

### 2.7 Microscopic observation

The collagen microspheres were fixed by 2.5% glutaraldehyde and were dehydrated by ethanol and subsequent isoamyl acetate. The samples were then freeze-dried and coated with Pt using an ion coater (L350S-C; Anelva, Japan) and subjected to SEM observation. The SEM apparatus (VE-9800; Kyence, Japan) was operated at 20 kV.

### 2.8 SDS- polyacrylamide gel electrophoresis (SDS-PAGE)

SDS-PAGE was performed by using an XV pantera system (DRC, Japan). The concentration of separation gel was 5%.



The collagen microspheres were mixed in diluted HCl (pH 3) to a final concentration of 10 mg/ml. Collagen and gelatin for controls were diluted in diluted HCl (pH 3) to a final concentration of 0.1% (w/v) and 1% (w/v), respectively. The samples were mixed with 0.1 M Tris-HCl buffer (pH 6.8) containing 69.3 mM SDS, 40% (v/v) glycerol, 0.7 mM bromophenol blue, and 10% (v/v) 2-mercaptoethanol at the ratio of 1: 1 (v/v), heat at 99°C for 5 min, and then 10  $\mu$ l was loaded per well of the XV pantera gel. After electrophoresis, gels were stained using 0.1% (w/v) Coomassie Brilliant Blue R250.

### 2.9 In vitro release study

The rhVEGF-loaded collagen microspheres (100 mg) were placed into insert wells (IntercellTP, Kurabo, Japan) and 400  $\mu$ l of solvents were added into lower wells of a 24-well plate (Asahi Techno Glass, Japan). As the solvents, PBS, collagenase solution in PBS (1 U/ml), and EGM were used. The collagen samples were incubated at a constant temperature of 37°C. After specific time periods, the solvents were collected and replaced with fresh solvents and incubated again. The content of rhVEGF released in the collected solvents was determined by a VEGF ELISA kit according to the manufacturer's instruction. To assess the degradability of the collagen microspheres in collagenase solution (1 U/ml) and PBS, protein content measurement was performed using a bicinchoninic acid protein assay kit as previously described [12].

### 2.10 Capillary formation assay

Capillary formation of the HUVECs co-cultured on NHDFs was assessed according to the method previously described [13]. Conditioned EGM containing released rhVEGF were prepared as follows; EGM were incubated with the rhVEGF-loaded collagen microspheres at a constant temperature of 37°C for a week and collected, followed by replacement with fresh EGM and incubation for another week. This procedure was repeated 3 times for 4 weeks. The HUVECs co-cultured with NHDFs were treated with the conditioned EGM at 37°C in air containing 5% CO<sub>2</sub>. As controls, fresh EGM and an EGM containing 2 nM (76.4 ng/ml) rhVEGF were used. At day 3 after the treatment, the cells were fixed and stained using an anti-human CD31 immunostaining kit according to the manufacturer's instruction. Stained area was calculated using an angiogenesis image analyzer (Kurabo).

### 2.11 Statistical analysis

Statistical analysis was performed using student's *t* tests, and a confidence level of 95% ( $P < 0.05$ ) was considered

necessary for statistical significance. The error bars indicate the standard deviation of the mean.

## 3 Results and discussion

### 3.1 Effect of surfactant concentration on particle size

Figure 1 shows the effect of surfactant concentration on the particle diameters. The average diameter, standard deviation, and variation coefficient were summarized in Table 1. The diameters proportionally decreased with increasing the surfactant concentration in the range of 0.1–0.5%. In this range, the diameters decreased at the ratio of 3.1  $\mu$ m per 0.1% increase of surfactant concentration. There was little change in diameter at concentrations of more than 0.5%. Meanwhile, absent surfactant resulted in increased particle diameter and standard deviation. Student's *t* tests showed that the surfactant concentration significantly influenced the particle size except the difference between 1 and 1.5%. Considering that removal of the surfactant from the microspheres was more complicated with increasing surfactant concentration and that the variation coefficient of the condition of 0.3% was the lowest, the optimal surfactant concentration was decided to be 0.3%.

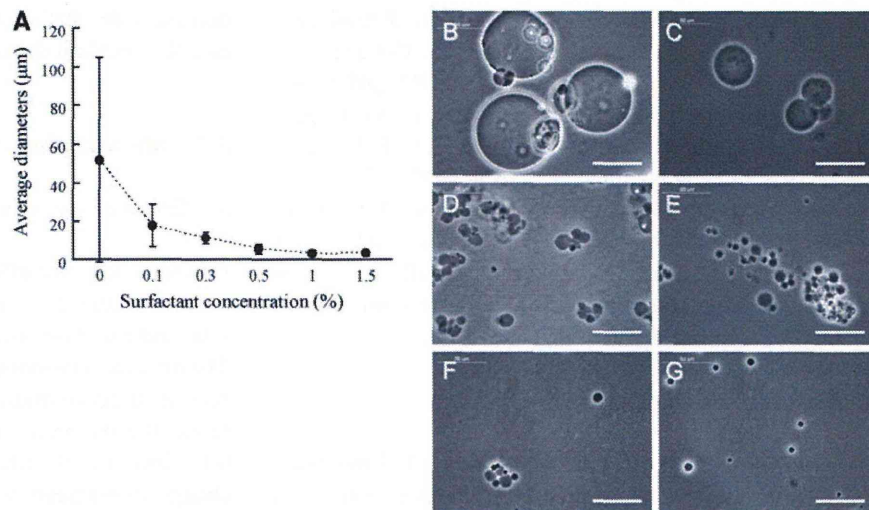
### 3.2 Effect of rotating speed on particle size

Figure 2 shows the effect of rotating speeds on the particle diameters under the condition of 0.3% surfactant concentration. The average diameter, standard deviation, and variation coefficient were summarized in Table 2. The diameters proportionally decreased with increasing the rotating speed at the ratio of 1.8  $\mu$ m per 100 rpm increase of the rotating speed, although the variation coefficient was the lowest at the rotating speed of 600 rpm. Student's *t* tests showed that the rotating speed significantly influenced the particle size. Consequently, the particle diameter could be controlled by changing the rotating speed and the rotating speed of 600 rpm was needed to make finer microspheres.

### 3.3 Effects of viscosity and temperature on particle size

Viscosity and reaction temperature of the emulsified mixture were important factors to control the particle size of the collagen microspheres. The viscosity of oil phase decreased with increasing temperature, although that of water phase showed little change (Fig. 3a). In addition, increased viscosity of oil phase resulted in decreased size of the particle diameter (Fig. 3b). It can be speculated that decreased viscosity of oil phase

**Fig. 1** Effect of surfactant concentrations on particle diameters (a). Photographs show the collagen microspheres prepared under the surfactant concentrations of 0% (b), 0.1% (c), 0.3% (d), 0.5% (e), 1% (f), and 1.5% (g), respectively. Rotating speed was set to 600 rpm. Bars: 50  $\mu\text{m}$



**Table 1** Effect of surfactant concentrations on diameter and dispersity of collagen microspheres

Surfactant concentration (%)	Average diameter ( $\mu\text{m}$ )	Standard deviation ( $\mu\text{m}$ )	Variation coefficient	Size range ( $\mu\text{m}$ )
0	51.68	53.14	1.028	5.26–315.7
0.1	17.77	11.27	0.634	2.65–71.43
0.3	11.38	3.16	0.278	3.36–21.01
0.5	5.49	2.58	0.470	1.68–16.81
1.0	3.21	1.63	0.508	0.84–12.61
1.5	3.36	1.53	0.455	0.42–10.92

**Fig. 2** Effect of rotating speeds in emulsion system on particle diameters (a). Photographs show the collagen microspheres prepared under the rotating speeds of 300 rpm (b), 600 rpm (c), 900 rpm (d), and 1,200 rpm (e), respectively. Surfactant concentration was set to 0.3%. Bars: 50  $\mu\text{m}$

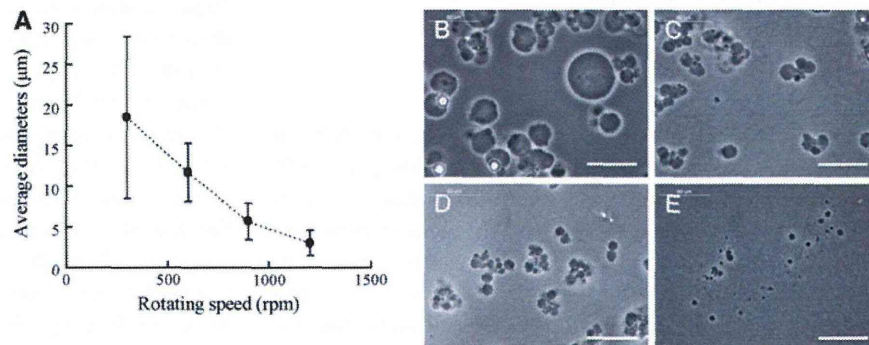


**Table 2** Effect of rotating speeds on diameter and dispersity of collagen microspheres

Rotating speed (rpm)	Average diameter ( $\mu\text{m}$ )	Standard deviation ( $\mu\text{m}$ )	Variation coefficient	Size range ( $\mu\text{m}$ )
300	18.51	9.92	0.536	2.63–92.11
600	11.73	3.60	0.307	2.52–25.21
900	5.71	2.25	0.394	0.84–11.76
1200	3.01	1.54	0.512	0.42–9.24

resulted in the formation of finer emulsion and larger droplets. On the other hand, increased collagen concentration of water phase also altered the particle diameters (Fig. 3c). The viscosity of collagen solution increased

with increasing the collagen concentration (Fig. 3a), therefore, the increased viscosity in water phase resulted in the increase of the particle diameter. Consequently, viscosity and temperature of the emulsified mixture